PAPER

α-Alkylidene δ-lactones inhibit quorum sensing phenotypes in *Chromobacterium* strain CV026 showing interaction with the CviR receptor†

Fernanda Favero,[ab] Terezinha Alves Tolentino,[a] Vinicius Fernandes,[c] Werner Treptow,*[c] Alex Leite Pereira*[b] and Angelo Henrique Lira Machado [ID] *[a]

Disruption of bacterial quorum sensing (QS) is presented as a promising strategy to overcome clinically relevant and phytopathogenic bacteria. This work presents α-alkylidene δ-lactones as new chemical scaffolds that inhibit the biosynthesis of violacein in the biosensor strain *Chromobacterium* CV026. Three molecules displayed higher than 50% violacein reduction when tested at concentrations lower than 625 μM. The most active α-alkylidene δ-lactone inhibited the hydrolysis of chitin concomitantly with the inhibition of violacein production in CV026, suggesting the disruption of its QS machinery. Further, RT-qPCR and competition experiments showed this molecule to be a transcriptional inhibitor of the QS-regulated operon *vioABCDE*. Docking calculations suggested a good correlation between binding affinity energies and inhibition effects, with all molecules positioned within the CviR autoinducer-binding domain (AIBD). The most active lactone yielded the best binding affinity energy, most probably due to its unprecedented binding with the AIBD. Our results show α-alkylidene δ-lactones as promising chemical scaffolds for the development of new QS inhibitors affecting LuxR/LuxI-systems.

Introduction

Lactones display several biological functions such as antimicrobial, antifungal, antiparasitic, anti-inflammatory, and cytotoxic, and others have been attributed to them.[1–6] They are usually secondary metabolites and can play several roles in cellular physiology, including cell–cell signalling such as Quorum Sensing (QS).[17] Bacteria produce chemical signals, called autoinducers (AI), to scan their population growth.[8–10] At a threshold concentration, an AI enables bacteria to synchronize changes in gene expression on a population scale, activating or repressing genes that benefit the survival of the community.

Several important biological processes have been described as being regulated by QS, including bioluminescence, virulence, and the synthesis of toxins and antibiotics. It is important to note that QS-controlled genes are essential for surveillance, survival, and adaptation to environmental changes.[7,11] Gram-negative bacteria use *N*-acyl homoserine γ-lactones (AHL) like

1 and 2 as autoinducers (Fig. 1a).[8] The AHL are synthesized by LuxI and recognized by LuxR-type proteins that act as transcription factors controlling QS genes. Homologs of the LuxI–
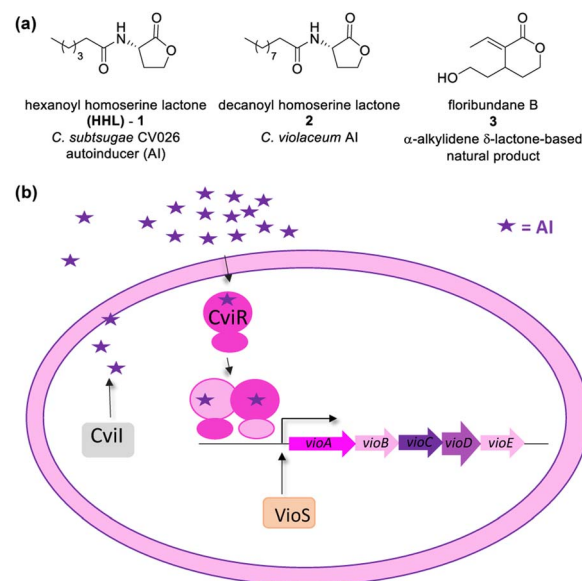
[a]Instituto de Química, Universidade de Brasília, Campus Universitário Darcy Ribeiro, Asa Norte, Brasília, DF, 70910-900, Brazil. E-mail: nagelo@unb.br

[b]Campus of Ceilândia, University of Brasília, Centro Metropolitano, Conjunto A, Ceilândia Sul, Brasília, DF, 72220-275, Brazil. E-mail: alexpereira@unb.br

[c]Laboratório de Biologia Teórica e Computacional, Departamento de Biologia Celular, Universidade de Brasília, Campus Universitário Darcy Ribeiro, Asa Norte, Brasília, DF, 70910-900, Brazil. E-mail: treptow@unb.br

† Electronic supplementary information (ESI) available. See DOI: https://doi.org/10.1039/d3ra01975f

Fig. 1 (a) Chemical structure of autoinducers (AI) of *Chromobacterium* spp. and an example of an α-alkylidene δ-lactone-based natural product. (b) CviI/R system present in *Chromobacterium violaceum* and *Chromobacterium subtsugae* strain CV026.

LuxR QS module occur in a variety of Gram-negative bacteria, including clinically relevant species (such as *Pseudomonas aeruginosa*, *Burkholderia cepacia*, *Aeromonas hydrophila*, *Chromobacterium violaceum*, *Yersinia* spp.) as well as in the phytopathogen *Agrobacterium tumefaciens*.[8,11]

Resistance to antibiotics is a challenge for public health. Approaches based on the inhibition of QS are promising therapies to control bacterial infections.[12–16] QS inhibitors (QSI) are supposed to cause a lower evolutionary pressure than antibiotics, leading to slower emergence of resistance.[17] QS inhibition can occur in three ways: the degradation of AI, the interruption of autoinducer biosynthesis, and the use of antagonists of the receptor proteins.[18]

In the literature, the chemical structure of AIs has been extensively used as the chemical scaffold for the synthesis of antagonists or LuxR-type proteins.[8,19] Natural products, such as flavonoids, flavones, and furanones, have already proven their effectiveness as QS inhibitors.[20–22]

CV026 is a model strain in QSI studies. It is known as an AHL-deficient mutant of *Chromobacterium* strain ATCC 31532 that has deleted the *luxI*-type gene *cviI*, and the *vioS*, the repressor gene of the CviI/R system.[23,24] CV026 only produces violacein in response to an externally supplied hexanoyl-L-homoserine lactone (HHL). *Chromobacterium* strains ATCC 31532 and CV026 were recently reclassified as *Chromobacterium subtsugae*.[25]

As in *C. violaceum*, QS in CV026 controls biofilm formation, chitinase enzymes, and violacein biosynthesis. A gene cluster found in an 8-kb DNA locus encodes the proteins of CV026 related to violacein biosynthesis as a single operon (*vioABCDE*). The CviR-trigged expression of *vioABCDE* produces large and polycistronic RNA transcripts that contiguously harbour the coding information for translation of the proteins involved in violacein biosynthesis (VioA, VioB, VioC, VioD, and VioE).[26,27] The production of this purple pigment is an easily quantifiable QS-regulated function.[23] The CviR of CV026 recognizes HHL (**1**) as an autoinducer, and that of *C. violaceum* recognizes decanoyl homoserine lactone (**2**) (Fig. 1a). The CviR–AI complex is an X-shaped homodimer that functions as a transcriptional activator controlling the expression of target genes.[13]

CV026 has been used in a screening assay to detect QS modulators that display an inhibitory effect on *C. violaceum* and *Pseudomonas aeruginosa* biofilms.[21,28,29] Arena and co-workers studied the effect of seven coumarin skeletons as inhibitors of biofilm and QS mechanisms in *C. violaceum* and *P. aeruginosa*.[30]

Blackwell and co-workers reviewed several compounds capable of modulating the QS in *P. aeruginosa*.[19] 5-Membered lactones are widely studied because they mimic molecular motifs held by the cognate AI. However, 6-membered lactones have been little explored as QS modulators. The α-alkylidene δ-lactones (**3**, Fig. 1a) are members of this chemical group that show significant biological activities.[31] The comparison of the α-alkylidene δ-lactone chemical structure with that of the AHLs allows one to highlight that the conformational restriction imposed by the alkylidene moiety can mimic the effect of the chirality at Cα and the exocyclic planar amide on positioning the side chain of the acyl moiety of the AHL within the

autoinducer-binding domain (AIBD) of CviR. To the best of our knowledge, the impact of this structural modification on the modulation of Gram-negative QS has not been evaluated so far. This work studied the effects of α-alkylidene δ-lactones against the QS of *C. subtsugae* strain CV026. Furthermore, this work probed the production of violacein, and the hydrolysis of chitin, well-known phenotypes of this QS system.[32] RT-qPCR and competitive assays were conducted to assess the impact of α-alkylidene δ-lactones on the expression of the CviR-controlled *vioABCDE* operon. Molecular docking calculations were conducted to evaluate the binding affinity of these lactones to CviR, and to probe their structure–activity relationships (SAR) as QSI.
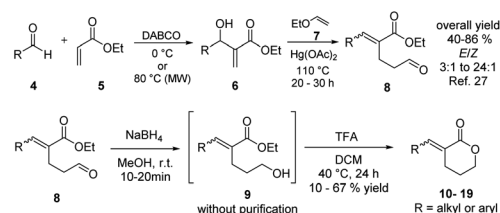
Results

Synthesis of the α-alkylidene δ-lactones

A representative library of α-alkylidene δ-lactones (**10–19**) was synthesized in good overall yields from the aldehydes **8** by their chemoselective reduction with sodium borohydride in methanol, followed by acidic cyclization without further purification (Scheme 1). The aldehydes **8** were obtained in a stereoselective way by a previously reported route of synthesis, starting from Morita–Baylis–Hillman adducts prepared with readily available aldehydes **4** and ethyl acrylate **5**.[33]

Synthesis of chlorolactone (20)

Chlorolactone (**20**) was synthesized by a synthetic route based on that proposed by Bassler and co-workers, as shown in the ESI (Scheme S1†).[34] This molecule is a known inhibitor of the CV026 QS and was used as a positive inhibition control to validate our biological evaluation.[13]

Biological evaluation

Violacein quantification assay. The δ-lactones were initially tested as possible QS inhibitors (QSI) of the strain CV026 by assaying their interference in the biosynthesis of violacein (Scheme S2†). The violacein quantification assay was performed under two conditions. In the one entitled "QSI test", the δ-lactone was added in different concentrations to bacterial culture, along with the cognate AI, to quantify the production of violacein. In the condition called "blank", it was evaluated whether concentrations of δ-lactone displaying a possible QSI effect were able to lessen microbial growth when compared to a parallel control culture without δ-lactones (solvent growth control). In the occurrence of any statistical difference ($p \leq 0.05$) between the blank condition and the growth control test, the


**Scheme 1** Synthetic route to compounds **10–19**.

respective QSI result was disregarded due to the inhibition of bacterial growth. Inhibitions in bacterial growth are indicated with asterisk-marked brackets plotted on the violacein quantification graphics. The percentual inhibition of violacein synthesis was calculated using eqn (1).

$$
\% \text{ (inhibition)} = (\mu \text{ODtest}_{\text{solvent}} - \mu \text{ODtest}_{\text{molecule}}) \\
\times 100\%/\mu \text{ODtest}_{\text{solvent}} \quad (1)
$$

Table 1 shows the violacein inhibition results achieved by δ-lactones. Some of them had their best percentages of inhibition at higher tested concentrations, but for comparison reasons here we show inhibition results at 625 μM. The complete set of inhibition results is found in the ESI (Fig. S1 to S15).†

Aliphatic lactones with longer chains delivered better inhibition values when compared to the short ones. **12E** (with 52% inhibition at a concentration of 1.25 mM, Fig. 2a) and **13E** (with 42% inhibition at a concentration of 1.25 mm, Fig. S7†). For the aromatic ones, the molecule **15E** showed inhibition of 75% and 85% at concentrations of 312 μM and 625 μM, respectively (Table 1 and Fig. 2b), achieving the best result among all the α-alkylidene δ-lactones. It is worth mentioning that the 2.5 and 1.25 mM concentrations were not considered, as they showed

Table 1 Data for inhibition of the violacein biosynthesis in *C. subtsugae* observed for α-alkylidene δ-lactones

Molecule		Inhibition (%) at 625 μM
	10E	10
	10Z	10
	11E	15
	11Z	20
	12E	42
	12Z	42
	13E	30
	13Z	40
	14E	18
	15E	85
	16E	55
	17E	60
	18E	35
	19E	35
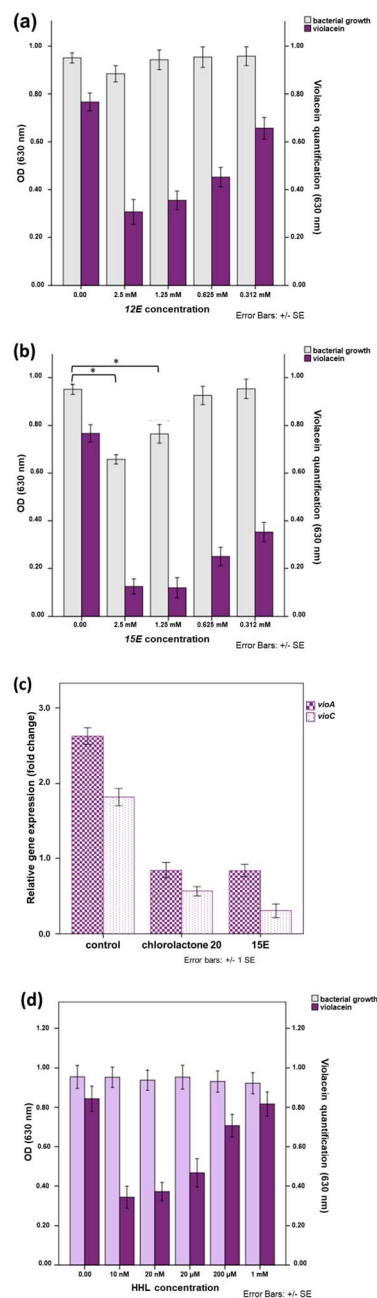
Fig. 2 The effect of α-alkylidene δ-lactones on violacein synthesis and genes which are under the control of QS. (a) Violacein quantification assay for the aliphatic lactone **12E**. (b) Violacein quantification assay for the aromatic lactone **15E**. Brackets marked with asterisks indicate conditions in which statistical differences in bacterial growth were observed when comparing the δ-lactone test with the growth control test. (c) RT-qPCR analysis showing the inhibitory effect of **20** (32.5 μM) and **15E** (312 μM) on the expression of the QS-regulated *vioABCDE* transcript (assessed by loci *vioA* and *vioC*). *gyrB* gene was used as an internal control for data normalization. (d) Competitive assay between autoinducer **1** (10 nM to 1 mM) and **15E** (312 μM).

a decrease in microbial growth. In the validation test with **20**, inhibition of the violacein biosynthesis by 95% was observed at a concentration of 32 μM (Fig. S15†). This result agreed with the previous one reported by Bassler for the inhibition of HHL-
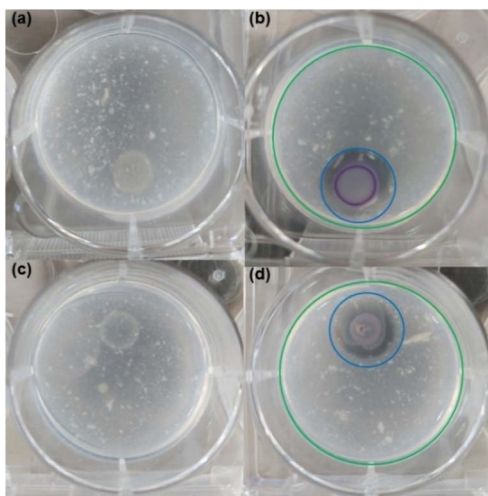
Fig. 3 Chitin hydrolysis induction test in CV026 strain. (a) Test conducted without exogenous autoinducer 1 (negative control). CV026 colony did not produce hydrolysis in the absence of the exogenous autoinducer or violacein pigment. (b) Test conducted with addition of autoinducer 1 (positive control). CV026 colony developed a clear chitin hydrolysis halo and violacein production. The extension of chitin hydrolysis is highlighted by a blue-outlined circle. (c) Inhibition of chitin hydrolysis and violacein production in test set up with the autoinducer 1 and QS inhibitor chlorolactone 20. (d) Inhibition of chitin hydrolysis and violacein production in test set up with the autoinducer 1 and lactone 15E. Green and blue-outlined circles in frames (b) and (d) have the same dimensions and were embedded in images to facilitate comparisons.

producing *C. subtsugae* strain CV31532, which showed IC50 = 2.6 μM.[34]

Chitinase assay. In *Chromobacterium* strain CV026, the hydrolysis of chitin is a phenotype controlled by QS. The chitinase assay developed by Chernin and co-workers was carried out to test the effect of the lactone 15E on chitinase activity.[32] Initially, it was shown that QS induction is needed for the expression of chitinase activity in CV026 strains (Fig. 3a and b). Upon QS induction (Fig. 3b) the CV026 colony displayed violacein pigmentation. Additionally, a clear halo was observed, revealing the hydrolysis of chitin induced by QS surrounding the violacein-pigmented colony. As expected, the colony of CV026 did not produce a hydrolysis halo and violacein when in the presence of the inhibitory control 20 (Fig. 3c). Lactone 15E also inhibited both QS phenotypes in CV026 (Fig. 3d), but with weaker activity.

RT-qPCR effect of lactone 15E on transcription of violacein synthesis related genes. RT-qPCR assays probing the target loci *vioA* and *vioC* were performed to investigate the effect of lactone 15E on the expression of the QS-regulated *vioABCDE* RNA transcript (Fig. 2c). The experiment with positive inhibition control 20 showed suppression of *vioABCDE* transcription. The expression of probed targets *vioA* and *vioC* decreased by 68% and 70% in the presence of 20, respectively. Lactone 15E delivered a similar inhibitory effect, with a reduction in the expression of the probed targets *vioA* and *vioC* of 68% and 80%, respectively.

Competition assay. Competition assays were performed with a fixed concentration of lactone 15E (312 μM) and increasing
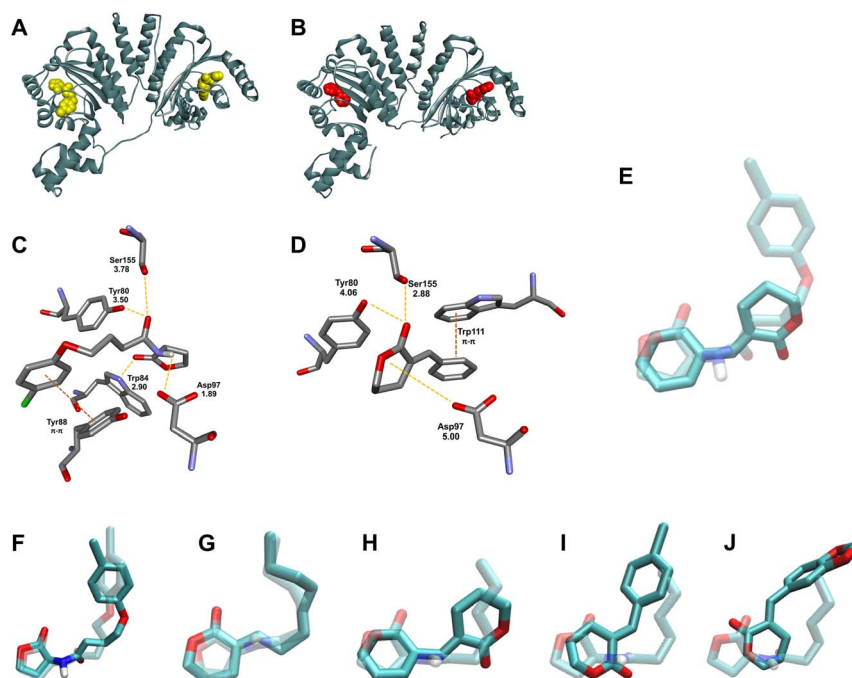
Fig. 4 Modeling studies of compounds 20, 15E and representative α-alkylidene δ-lactones docked into the active site of CviR (PDB ID 3PQ5). (A) Structure of the CviR : 20 complex yielded by redocking (20 is highlighted in gold). (B) Docked structure of the CviR : 15E complex (15E is highlighted in red). (C) Compound 20 in the AIBD of CviR. (D) Compound 15E in the AIBD of CviR. (E) Comparison of the binding mode of the docked 20 overlapped with 15E in the binding domain. (F) Comparison of the binding mode of the crystallographic (dashed) and redocked (solid) 20. Comparison of the binding mode of the docked autoinducer 1 (dashed) and representative α-alkylidene δ-lactones: (G) 12E, (H) 15E, (I) 16E, and (J) 18E.

Table 2 Data for interactions between α-alkylidene δ-lactones and CviR observed by molecular docking

Molecule	Binding affinity (kcal mol^{-1})	Hydrophilic interaction (H-bond)[a]	Hydrophobic interactions	logP
HHL (**1**)	−7.0	Tyr80, Trp84, Tyr88, Asp97, Ser155	—	0.952
Positive inhibition control (**20**)	−8.8	Tyr80, Trp84, Tyr88, Asp97, Ser155	Tyr88	1.474
Negative inhibition control (**21**)	0.0	No interactions within the AIBD	No interactions within the AIBD	4.787
10E	−6.2	Trp84, Asp97, Ser155	—	1.665
10Z	−6.4	Trp84, Asp97, Ser155	—	1.665
11E	−6.5	Tyr80, Trp84, Tyr88, Asp97, Ser155	—	2.110
11Z	−6.3	Tyr80, Trp84, Tyr88, Asp97, Ser155	—	2.110
12E	−7.0	Tyr80, Trp84, Ser155	—	3.444
12Z	−7.4	Tyr80, Trp84, Asp97	—	3.888
13E	−7.4	Tyr80, Trp84, Asp97	—	4.333
13Z	−7.5	Tyr80, Trp84, Asp97	—	4.333
14E	−6.5	Tyr80, Asp97, Ser155, Trp111, Thr140	—	2.397
15E	−8.4	Tyr80, Tyr88, Asp97, Ser155	Trp111	2.882
16E	−8.3	Tyr88, Asp97, Ser155, Trp111	Tyr88	3.486
17E	−8.1	Tyr88, Asp97, Ser155, Leu85[b], Trp111	Tyr88	3.651
18E	−8.5	Trp84, Asp97, Asn77	—	2.526
19E	−8.0	Trp84, Asp97, Asn77	—	2.505

[a] Amino acid residues highlighted are non-coincidental to CviR : HHL (**2**) complex. [b] Non-conventional H-bond.

concentrations of the cognate autoinducer **1** (ranging from 10 nM to 1 mM) to verify if violacein inhibition could be released (Fig. 2d). The results showed a dose-dependent pattern, while violacein production was restored by increasing the autoinducer concentration. It is important to note that the full restoration in violacein production was achieved as the autoinducer reached a concentration similar to that used for **15E** (autoinducer **1** above 200 μM) (Fig. 2d), and this concentration corresponds to 10 000 times the natural activation dose of the HHL.[13] These results suggested that autoinducer **1** and lactone **15E** act as competitive antagonists.

Molecular docking and logP calculations. Molecular docking studies[35] and the theoretical calculation of logP[36] were performed to uncover the relationships between the structure of α-alkylidene δ-lactones and their inhibitory activities. Blind docking experiments were computed with CviR (PDB ID 3QP5) and the ligands studied here.[13] Interactions were considered when the distance between the atoms was equal to or less than 5 Å. The blind redocking for the CviR/**20** complex showed **20** positioned at the CviR AIBD, in a pose that matched the one observed in crystallographic data (Fig. 4A, C, and F). This experiment also showed that the most important interactions between positive inhibition control **20** and the AIBD are with Tyr80, Trp84, Tyr88, Asp97, and Ser155 residues, and the π–π stacking between its aromatic ring and Tyr88 (Fig. S17†). The binding energy computed for this complex was −8.8 kcal mol^{-1}. For cognate AI **1**, these interactions were maintained, except for the π–π stacking (Fig. S16†). This complex has an interaction energy of −7.1 kcal mol^{-1}. Blind docking experiments showed that the α-alkylidene δ-lactone **15E** had favourable interactions with the residues Tyr80, Asp97, Trp111, and Ser155, displaying similar interactions to those contacted by **20** (Tyr80, Asp97, Ser155) (Fig. 4B, D, E and H). Additionally, **15E** maintained a π–π stacking interaction with the

residue Trp111. The binding energy computed for the complex CviR/**15E** was −8.4 kcal mol^{-1} (Table 2). The molecular docking experiments performed with all the α-alkylidene δ-lactones showed interaction with the AIBD as their most stable pose. Their binding affinity energy and the amino acid residues that interact with each lactone are reported in Table 2. A comprehensive discussion of the impact of these interactions on inhibitory activity can be found as part of the following section.

To summarize this information, we plotted logP, inhibition percentage, and normalized docking energy on a single 3D graphic (Fig. 5). The docking energies were normalized by the lowest value computed, which corresponds to positive inhibition control **20**. For comparison purposes, we chose a molecule from Fallarero's work (**21**, Fig. S32†) as a negative inhibition control.[21] It did not affect violacein biosynthesis at 400 μM and its calculated logP is 4.787.

Discussion

The α-alkylidene δ-lactones here investigated were tested for their ability to interfere with violacein biosynthesis, with all of them displaying an inhibitory effect around 625 μM. The biosynthesis of violacein is a well-known QS-regulated phenotype in strain CV026 and can be described as a two-step event: (a) the transcription of the *vioABCDE* genes allowing the production of the enzymes responsible for violacein biosynthesis; and (b) the transformation of tryptophan into violacein accomplished by the *vioABCDE* metabolic pathway.[26] Starting from this premise, the inhibition of violacein biosynthesis observed for the α-alkylidene δ-lactones could come independently from (1) the disruption of the transcriptional event mediated by CviR or (2) the antagonist action of these lactones in one of the biosynthetic steps catalysed by *vioABCDE* enzymes.
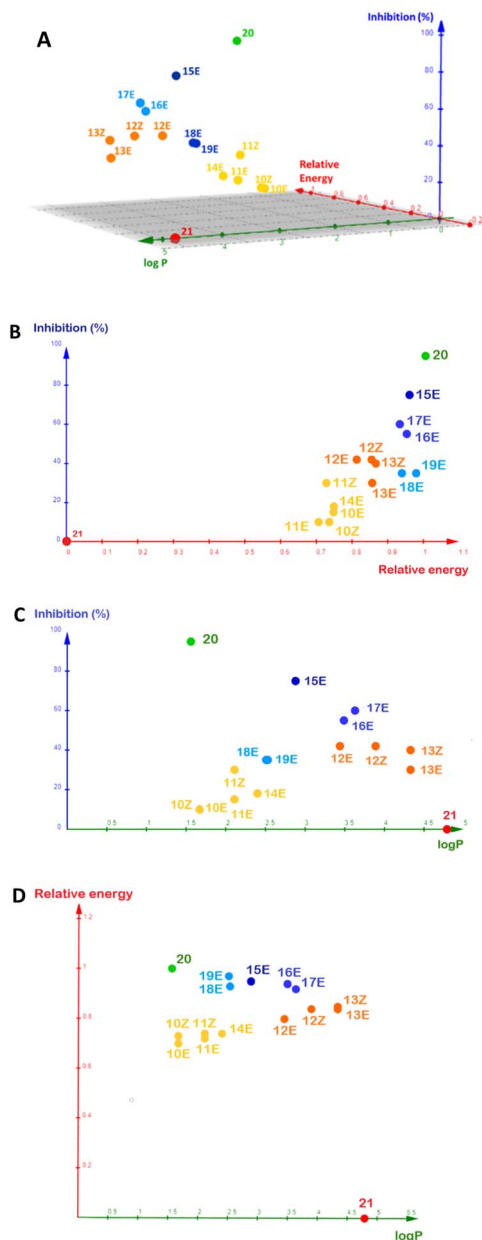
Fig. 5 Comparative analysis of the contribution of the relative docking energy and logP to the inhibition (%) observed for positive control **20**, for α-alkylidene δ-lactones **10–19** (at a concentration of 312 μM) and negative control **21** (at a concentration of 400 μM). Relative docking energies were computed by blind docking. (A) 3D plot of the variation of the inhibition (%) against logP and relative docking energy. (B) Isolated view of the inhibition (%) against relative docking energy. (C) Isolated view of the inhibition (%) against logP. (D) Isolated view of the relative docking energy against logP.

The chemical structure of the α-alkylidene δ-lactones is similar to the one of AHL **1**, the cognate autoinducer of the CV026 QS. They have a hydrophilic lactone attached at Cα to a lipophilic hydrocarbon side chain, and this chemical similarity prompted us to suggest that the inhibitory profile observed for the α-alkylidene δ-lactones could be due to the competitive antagonist binding of these lactones to the CviR AIBD, disrupting the QS in CV026.

Lactone **15E** showed the best inhibition of violacein biosynthesis in CV026, 85% at concentrations of 625 μM, and was selected for further investigation of the origin of the α-alkylidene δ-lactone's inhibitory activity here observed. In a competitive binding assay with **15E** and cognate autoinducer **1**, a complete restoration of violacein production was achieved as the autoinducer concentration reached similar values to those used for **15E**. Additionally, RT-qPCR experiments with **15E** showed a decrease in the expression of *vioABCDE* RNA transcripts. These results characterize it as a QSI that works at the transcriptional level.

The α-alkylidene δ-lactone **15E** also inhibited hydrolysis of chitin, a well-known QS-regulated phenotype in strain CV026, concomitantly with the suppression of violacein biosynthesis.[16] This result was observed similarly to that for QS inhibitor **20**, endorsing the initial hypothesis that, at the transcriptional level, α-alkylidene δ-lactones can inhibit the AHL-based QS in CV026.

The blind molecular docking studies conducted with the CviR crystal structure (PDB ID 3QP5) were used here to evaluate if and how these new QSI α-alkylidene δ-lactones interact with CviR. All tested δ-lactones showed interaction with the AIBD of CviR as their most stable pose (Fig. S18–S31†). The molecular docking energies computed for the δ-lactones ranged from -6.2 kcal mol^{-1} to -8.5 kcal mol^{-1} (Table 2), with a similar magnitude to that computed for cognate AI **1**, (-7.0 kcal mol^{-1}) and positive inhibition control **20** (-8.8 kcal mol^{-1}). Negative control **21** could not be found in the AIBD, and relative energy equal to zero was assigned to it (Fig. S32†).

In addition to the similar docking energies shown by **20** and **15E** (respectively, -8.8 kcal mol^{-1} *vs.* -8.4 kcal mol^{-1}), these QS inhibitors share four hydrophilic interactions in the CviR AIBD. Docking information, together with RT-qPCR results and the competition assay, endorse the hypothesis that the observed QS inhibition caused by **15E** occurs due to the competition between this δ-lactone and cognate autoinducer **1** to bind CviR, inhibiting the expression of the *vioABCDE* operon at the transcriptional level in CV026.

The logP of the α-alkylidene δ-lactones was calculated (Table 2), and all values were lower than 5, suggesting their ability to diffuse across the bacterial membrane.[36] However, the logP could not be assigned as a good descriptor for the analysis of SAR regarding the inhibition measured for these δ-lactones (Fig. 5d). The aliphatic lactones showed logP ranging from 1.6–4.3, and those with the best inhibition – namely **12E**, **12Z**, **13E**, and **13Z** – had the logP > 3.000, far from the positive inhibitory control **20** (logP = 1.474). A different trend was observed for the aromatic δ-lactones. Their logP varied over a much smaller range, between 2.501 and 3.651, when compared to the aliphatic ones. These values were closer to the logP for positive inhibitory control **20**, suggesting that the presence of the phenyl group, substituted or not, improves the inhibitory activity.

To evaluate the correlation between the interaction energies obtained by docking and the per cent inhibition, these energies were normalized by the one computed for complex CviR : **20**. In contrast to the logP, relative interaction energy and QS inhibition percentage had a good correlation, as can be seen in Fig. 5b.

Hughson, Bassler and co-workers introduced a seminal discussion concerning the CviR conformational changes imposed by the acyl chains of AHL-based ligands.[13] Long-chain AHLs showed competitive inhibitory activity on this enzyme. To better understand this fact at the molecular level, they analysed the X-ray crystal structure of the CviR complexed with different AHLs, including **1**, **2**, AHL with C8 acyl side chain, and aromatic analogue **20**. Those that showed inhibitory activity had the acyl side chain oriented toward Met 89, resulting in conformational changes for CviR that prevented interaction with the DNA, thereby inhibiting the transcription of *vioABCDE*. Our results corroborate this discussion, because the α-alkylidene δ-lactones with longer aliphatic chains yielded better inhibition results for those with alkyl ones (**10–13**), in addition to better relative interaction energies (Fig. 5c). These findings prompted us to suggest that longer aliphatic side chains, in addition to the increase in the permeability of the lactones through the cell envelope and their cellular concentration, optimize the inter-action with the AIBD to promote the conformational changes in CviR needed to prevent its interaction with DNA, in a way similar to that proposed by Hughson, Bassler and co-workers for the AHL inhibitors (Fig. 4g).

The behaviour of the docking results for the aromatic δ-lactones in the AIBD was less convergent than that for those with alkyl side chains. Compounds **15E–18E** were positioned with their lactone moiety in the same AIBD region where the homoserine lactone of the AHLs would be, with the benzylidene group oriented toward the same AIBD region occupied by the aryl group of **20**. This pose suggests the same π–π stacking interaction with Trp88 observed for this known inhibitor. Despite this similarity between these four δ-lactones, the C=O for **17E** and **18E** was pointed toward the Trp84 residue of CviR (Fig. 4J and S30,† respectively), in contrast to **15E** and **16E**, which had their carbonyl oriented to the opposite direction, making a hydrogen bond with Tyr88 (Fig. 4I and, S28,† respectively). These differences did not impose significant changes on their docking energy, but they did seem to affect their inhibitory activity on violacein biosynthesis.

A particular difference in the binding pose for α-benzylidene δ-lactone **15E** is noteworthy. Its lactone ring was found posi-tioned at the same AIBD region occupied by the AHL's acyl chain, and its aromatic moiety was oriented toward the same AIBD region occupied by the AHL's homoserine lactone (Fig. 4H and S27†). This unprecedented docking pose positioned the phenyl ring of the δ-lactone **15E** parallel to the Trp111 residue, suggesting π–π stacking, which, to the best of our knowledge, has never been reported before for lactone-based CviR ligands.

A comparison of the inhibition measured for the α-benzyli-dene δ-lactones, their relative docking energies, and log*P* (Fig. 5) endorses the binding pose of **15E** at the AIBD as the basis for its inhibitory effect.

Conclusion

A representative library of compounds belonging to α-alkyli-dene δ-lactones was evaluated for their inhibitory activity for violacein production in a *C. subtsugae* CV026 bioassay. Out of the 14 compounds, two (**12E** and **15E**) proved to be the most promising ones. The competitive binding assay between **15E** and cognate autoinducer **1** showed a dose-dependent pattern, while violacein production was gradually restored by increasing the concentration of autoinducer **1**. Lactone **15E** also inhibited the chitin hydrolysis concomitantly with violacein production in a *C. subtsugae* CV026 bioassay; both are well-known QS-mediated phenotypes, suggesting that this α-alkylidene δ-lactone is working at a transcriptional level, disrupting the CV026 QS machinery. RT-qPCR experiments with **15E** showed a decrease in the expression of *vioABCDE* RNA transcripts assessed *via* two target loci (*vio*A and *vio*C with 68% and 80% decrease, respectively). These results characterize **15E** as a QSI that works at the transcriptional level in CV026. Docking studies for the α-alkylidene δ-lactones with CviR suggested that molecular interactions of the lactone moiety with AIBD can mimic the interactions of lactone **1**. The aromatic lactones have π–π stacking interaction that improves their binding with the CviR protein. The most active compound, **15E**, showed the best binding affinity by docking studies, most probably due to its unprecedented binding positioning with the AIBD. The original hypothesis that motivated the evaluation of α-alkylidene δ-lactones as modulators of the QS in CV026 was based on the structural similarity between them and the cognate AI, sug-gesting that α-alkylidene δ-lactones could mimic the AI pose within the CviR AIBD. Surprisingly, blind docking calculations for CviR : **15E** complex yielded the ligand positioned within the CviR AIBD but inverted with respect to the cognate AI, with the phenyl group of **15E** fitting the AI's lactone pocket, and the lactone ring of **15E** filling the AI's acyl chain pocket. Although this pose seems divergent from our original hypothesis, lactone **15E** presents interactions with the same amino acid residues that are functionally important for QS inhibition, in agreement with the inhibition mechanism proposed by Hughson and Bassler for *Chromobacterium* spp.[13] Taken together, these docking calculations suggest that the shortening of the spacer between the lactone and the aryl ring still allows **15E**-like molecules to block the CviR AIBD by a molecular binding mechanism distinct from classic AHL-based inhibitors such as the inhibitor **20** proposed by Bassler. This study shows that the α-alkylidene δ-lactone is a new chemical scaffold with the potential to act as a QSI in Gram-negative LuxR/LuxI-type QS systems, and further studies are ongoing in our group to explore them in searching for novel optimized QSIs.

Experimental section

Chemistry

Solvents obtained from commercial sources were treated, before being used, according to procedures previously described in the literature. Anhydrous DMF was purchased from Sigma-Aldrich in a sure-seal flask. Nuclear magnetic resonance (NMR) experiments were performed on the following devices: Varian Mercury Plus (300 MHz for ^{1}H and 75 MHz for ^{13}C) 7.04 T and Bruker Ascend (600 MHz for ^{1}H 150 and MHz for ^{13}C) 14.1 T. chemical shifts (δ) were expressed in parts per million (ppm). Coupling constants are expressed in Hertz (Hz).

The analysed samples were dissolved in deuterated chloroform (CDCl$_3$). For ^{1}H NMR spectra, TMS tetramethylsilane (0.00 ppm) was used as an internal reference, and for ^{13}C NMR spectra, deuterated chloroform (77.0 ppm). The spectra were processed using the MestreNova 6.0 program.

QSI synthesis

The α-alkylidene δ-lactones of this study were synthesized as described by Machado and co-workers.[33]

General procedure for Hurd–Claisen rearrangement of Morita–Baylis–Hillman (MBH) adducts 6. In a Schlenk flask were added the MBH adduct **6** (2.5 mmol), ethyl vinyl ether **7** (13 mmol) and mercury acetate (2.5 mol%). The mixture was kept at 110 °C under stirring for 24–30 h. Crude aliquot reactions were analysed by ^{1}H NMR for conversion and selectivity calculation. The reaction was then treated with 7.5 mL of ethyl ether and washed with brine (3 × 5 mL). The organic phase was dried over MgSO$_4$, filtered, and concentrated *in vacuo*. The residue was purified by flash column chromatography on silica gel (10% ethyl acetate in hexane (v/v) as the eluent solution) to furnish the desired product.

Ethyl (E/Z)-2-ethylidene-5-oxopentanoate (8; R = Me mixture of isomers). Physical state: light yellow oil. Yield: 86% (E/Z 3.0 : 1.0). ^{1}H NMR (600 MHz, CDCl$_3$, 25 °C) δ 9.78 (t, J = 1.5 Hz, 1H), Z 9.76 (t, J = 1.3 Hz, 1H), E 6.92 (q, J = 7.2 Hz, 1H), Z 6.11 (q, J = 7.2H, 1H), E 4.24–4.17 (m, 2H), E/Z 2.65–2.56 (m, 4H), Z 1.99 (d, J = 7.2 Hz, 3H), E 1.84 (d, J = 7.2 Hz, 3H), E/Z 1.33–1.27 (m, 3H). ^{13}C NMR (75 MHz, CDCl$_3$, 25 °C) δ E 201.7, 167.2, 138.6, 131.4, 60.5, 43.0, 14.2. Z 201.7, 167.4, 138.6, 130.9, 60.2, 43.4, Z 14.3, E/Z 19.2. MS (70 eV) m/z: (M)$^+$ 170, 41(100) IR (ATR): 2984, 1715, 1448, 1379, 1263, 1182. HRMS (ESI-TOF): [M + Na]$^+$ calcd for C$_9$H$_{14}$NaO$_3$ 193.0835, found 193.0831.

Ethyl (E/Z)-2-(3-oxopropyl)pent-2-enoate (8; R = Et mixture of isomers). Physical state: colorless oil. Yield: 67% (E/Z 3.0 : 1.0). ^{1}H NMR (600 MHz, CDCl$_3$, 25 °C) δ 9.78 (t, J = 1.4 Hz, 1H), Z 9.77 (t, J = 1.4 Hz, 1H), E 6.81 (t, J = 7.6 Hz, 1H), Z 5.97 (t, J = 7.4 Hz, 1H), E/Z 4.24–4.17 (m, 2H), E/Z 2.66–2.55 (m, 2H), E/Z 2.26–2.19 (m, 2H), E/Z 1.33–1.28 (m, 3H), E/Z 1.08–1.00 (M, 3H). ^{13}C NMR (75 MHz, CDCl$_3$, 25 °C) δ E 201.7, 145.4, 129.8, 60.5, 43.3, 21.8, 13.2. Z 201.7, 145.6, 129.7, 60.5, 43.4, 21.9, 13.2, E/Z 167.4, E/Z 19.4. IR (KBr): 2976; 2729; 1709; 1644; 1461; 1372; 859. HRMS (ESI-TOF): [M + H]$^+$ calcd for C$_{10}$H$_{17}$O$_3$ 185.1172, found 185.1180.

Ethyl (E/Z)-4-methyl-2-(3-oxopropyl)pent-2-enoate (8; R = iPro mixture of isomers). Physical state: colorless oil. Yield: 67% (E/Z 7.1 : 1.0). ^{1}H NMR (600 MHz, CDCl$_3$, 25 °C) δ E 9.74 (t, J = 1.4 Hz, 1H), Z 9.72 (t, J = 1.5 Hz, 1H), E 6.57 (d, J = 10.2 Hz, 1H), Z 5.69 (dd, J = 9.8 Hz, 1H), E/Z 4.19–4.12 (m, 2H), E/Z 2.66–2.50 (m, 5H), E/Z 1.28–1.18 (m, 3H), E 0.99 (d, J = 6.6 Hz, 6H), Z 0.94 (d, J = 6.6 Hz, 6H). ^{13}C NMR (151 MHz, CDCl$_3$, 25 °C) δ E 201.7, 167.6, 128.1, 60.6, 43.7, 22.2, 14.2, E/Z 150.4, E/Z 27.9, E/Z 19.6, Z 201.6, 167.5, 127.8, 176.5, 60.3, 43.5, 22.2, 14.2. MS (70 eV) m/z: 198 (M$^+$), 81 (100). IR (ATR): 2964, 2869, 1708, 1645, 1448, 1313, 1256. HRMS (ESI-TOF): [M + H]$^+$ calcd for C$_{11}$H$_{19}$O$_3$ 199.1329, found 199.1337.

Ethyl (E/Z)-2-(3-oxopropyl)non-2-enoate (8; R = Hex mixture of isomers). Physical state: colorless oil. Yield: 80% (E/Z 4.0 : 1.0).

^{1}H NMR (600 MHz, CDCl$_3$, 25 °C) δ E 9.78 (t, J = 1.4 Hz, 1H), Z 9.77 (t, J = 1.4 Hz, 1H), E 6.82 (t, J = 7.6 Hz, 1H), Z 5.99 (t, J = 7.4 Hz, 1H), E/Z 4.23–4.17 (m, 2H), E/Z, 2.64–2.55 (m, 4H), E/Z 2.22–2.17 (m, 2H), E/Z 1.48–1.21 (m, 11H), E/Z 0.90–0.86 (m, 3H). ^{13}C NMR (151 MHz, CDCl$_3$, 25 °C) δ E 201.6, 167.3, 144.2, 130.2, 60.5, 43.3, 31.7, 29.3, 29.0, 28.60, 22.6, 14.0, E/Z 19.5, E/Z 14.2, Z 201.7, 167.3, 144.3, 129.8, 60.2, 43.5, 31.7, 29.3, 28.9, 28.5, 22.5, 14.0. MS (70 eV) m/z: 240 (M$^+$), 137 (100). IR (ATR): 2925, 2865, 2858, 1708, 1456, 1363, 1270, 1183. HRMS (ESI-TOF): [M + H]$^+$ calcd for C$_{14}$H$_{25}$O$_3$ 241.1798, found 241.1800.

Ethyl (E/Z)-2-(3-oxopropyl)dec-2-enoate (8; R = Hept mixture of isomers). Physical state: colorless oil. Yield: 96% (E/Z 3.5 : 1.0). ^{1}H NMR (600 MHz, CDCl$_3$, 25 °C) δ E 9.77 (t, J = 1.4 Hz, 1H), Z 9.75 (m, 1H), E 6.80 (t, J = 7.6 Hz, 1H), Z 5.97 (t, J = 7.4 Hz, 1H), E/Z 4.24–4.11 (m, 2H), E/Z 2.65–2.50 (m, 4H), Z 2.42 (q, J = 7.3 Hz, 2H), E 2.15 (q, J = 7.3 Hz, 2H), E/Z 1.48–1.10 (m, 10H), E/Z 0.95–0.75 (m, 6H). ^{13}C NMR (151 MHz, CDCl$_3$, 25 °C) δ Z 201.8, E 201.7, Z 167.5, E 167.4, Z 144.4, E 144.2, E 130.3, Z 129.8, E 60.5, Z 60.2, Z 43.5, E 43.4, Z 31.8, E 31.7, Z 29.7, E 29.4, E 29.3, E 29.1, Z 28.8, E 28.7, E 28.6(3), Z 28.5(8), Z 27.4, Z 22.6, Z 22.1, E 19.6, E/Z 14.3, E/Z 14.1. MS (70 eV) m/z: 254 (M$^+$), 137 (100). IR (ATR): 2959, 2932, 2851, 1717, 1643, 1456, 1368, 1256, 1188. HRMS (ESI-TOF): [M + Na]$^+$ calcd for C$_{15}$H$_{27}$O$_3$ 255.1955, found 255.1948.

Ethyl (E)-2-benzylidene-5-oxopentanoate (8; R = Ph). Physical state: light green oil. Yield: 67% (E/Z 24.0 : 1.0). ^{1}H NMR (600 MHz, CDCl$_3$, 25 °C) δ 9.74 (t, J = 1.4 Hz, 1H), 7.72 (s, 1H), 7.38–7.25 (m, 5H), 4.25 (q, J = 7.1 Hz, 2H), 2.85–2.81 (m, 2H), 2.67–2.63 (m, 2H), 1.32 (t, J = 7.1 Hz, 3H). ^{13}C NMR (151 MHz, CDCl$_3$, 25 °C) δ 201.3, 167.7, 140.3, 135.3, 131.4, 129.0, 128.7, 128.6, 61.0, 43.2, 20.3, 14.3. MS (70 eV) m/z: 232 (M$^+$), 129 (100). IR (ATR): 2979, 2738, 1701, 1627, 1488, 1365. HRMS (ESI-TOF): [M + Na]$^+$ calcd for C$_{14}$H$_{16}$NaO$_3$ 255.0992, found 255.0990.

Ethyl (E)-2-(4-bromobenzylidene-5-oxopentanoate) (8; R = 4-Br-Ph). Physical state: colorless oil. Yield: 40% (E/Z 17.0 : 1.0). ^{1}H NMR (600 MHz, CDCl$_3$, 25 °C) δ 9.77 (t, J = 1.3 Hz, 1H), 7.65 (s, 1H), 7.54–7.51 (m, 2H), 7.21–7.17 (m, 2H), 4.28 (q, J = 7.1 Hz, 2H), 2.85–2.81 (m, 2H), 2.70–2.66 (m, 2H), 1.35 (t, J = 7.1 Hz, 3H). ^{13}C NMR (151 MHz, CDCl$_3$, 25 °C) δ 201.0, 167.5, 138.9, 134.1, 132.1, 130.5, 122.9, 61.2, 43.0, 20.2, 14.3. MS (70 eV) m/z: 310 (M$^+$), 129(100). IR (ATR): 2979, 1702, 1673, 1585, 1481, 1369. HRMS (ESI-TOF): [M + H]$^+$ calcd for C$_{14}$H$_{16}$BrO$_3$ 311.0277, found 311.0287.

Ethyl (E)-2-(4-chlorobenzylidene-5-oxopentanoate) (8; R = 4-Cl-Ph). Physical state: colorless oil. Yield: 73% (E/Z 18.0 : 1.0). ^{1}H NMR (300 MHz, CDCl$_3$, 25 °C) δ 9.78 (t, J = 1.3 Hz, 1H), 7.68 (s, 1H), 7.40–7.23 (m, 5H), 4.28 (q, J = 7.1 Hz, 2H), 2.87–2.78 (m, 2H), 2.73–2.65 (m, 2H), 1.35 (t, J = 7.1 Hz, 3H). ^{13}C NMR (151 MHz, CDCl$_3$, 25 °C) δ 201.2, 167.3, 139.1, 134.6, 133.4, 133.7, 132.1, 130.4, 128.9, 61.3, 43.0, 20.4, 14.4. MS (70 eV) m/z: 266 (M$^+$), 129 (100) IR (ATR): 2984, 2724, 1702, 1635, 1592, 1492, 1256, 1166. HRMS (ESI-TOF): [M + H]$^+$ calcd for C$_{14}$H$_{16}$ClO$_3$ 267.0782, found 267.0786.

Ethyl (E)-2-(4-nitrobenzylidene-5-oxopentanoate) (8; R = 4-NO$_2$-Ph). Physical state: yellow oil. Yield: 71% (E/Z 6.0 : 1.0). ^{1}H NMR (600 MHz, CDCl$_3$, 25 °C) δ Z 9.80 (s, 1H), E 9.73 (s, 1H), E 8.23 (d, J = 8.7 Hz, 2H), Z 8.13 (d, J = 8.7 Hz, 2H), E 7.71 (s, 1H), E 7.45 (d,

J = 8.8 Hz, 2H), Z 7.34 (d, J = 8.8 Hz, 2H), Z 6.76 (s, 1H), E 4.27 (q, J = 7.1 Hz, 2H), Z 4.10 (q, J = 7.1 Hz, 2H), E/Z 2.81–2.76 (m, 2H), E/Z 2.76–2.71 (m, 4H), E 2.68 (t, J = 7.6 Hz, 2H), Z 1.33 (t, J = 7.1 Hz, 3H), Z 1.08 (t, J = 7.1 Hz, 3H). ^{13}C NMR (151 MHz, CDCl$_3$, 25 °C) δ E 200.4, E/Z 166.9, E/Z 147.5, E/Z 141.9, E/Z 137.6, E 129.7, E 123.9, E 61.5, E 42.9, E/Z 27.8, E/Z 14.3, Z 200.4, Z 167.9, Z 129.0, Z 123.4, Z 61.2, 42.4, E/Z 20.3. HRMS (ESI-TOF): [M + H]$^+$ calcd for C$_{14}$H$_{16}$NO$_5$ 278.1023, found 278.1042.

Ethyl (E)-2-(benzo[d][1,3]dioxol-5-ylmethylene)-5-oxopentanoate (8; R = 3,4-(O-CH₂-O)-Ph). Physical state: yellow oil. Yield: 75% (E/Z 16.0 : 1.0). ^{1}H NMR (600 MHz, CDCl$_3$, 25 °C) δ 9.76 (t, J = 1.4 Hz, 1H), 7.63 (s, 1H), 6.82–6.78 (m, 4H), 5.96 (s, 2H); 4.23 (q, J = 7.1 Hz, 2H), 2.89–2.81 (m, 2H), 2.67–2.63 (m, 2H), 1.30 (t, J = 7.1 Hz, 3H). ^{13}C NMR (151 MHz, CDCl$_3$, 25 °C) δ 201.2, 168.1, 148.0, 139.9, 130.1, 129.2, 124.0, 109.0, 108.6, 101.4, 61.0, 43.1, 20.3, 13.9. MS (70 eV) *m/z*: 276 (M$^+$), 115 (100). IR (ATR): 2978, 2896, 1702, 1623, 1494, 1446, 1365. HRMS (ESI-TOF): [M + H]$^+$ calcd for C$_{15}$H$_{17}$O$_5$ 277.1071, found 277.1071.

General procedure for the synthesis of the alkylidene lactones. To a solution of an aldehyde **8** (1.0 mmol of aldehyde) in 10 mL of absolute ethanol was slowly added 2.0 mmol of sodium borohydride, at 0 °C. The reaction mixture was magnetically agitated until the reagent was consumed when monitored by TLC. This time varied between 10 and 20 minutes. After checking the consumption of the aldehyde, 1% HCl was added dropwise until pH = 2–3. The reaction medium was then neutralized with the addition of saturated sodium bicarbonate solution. The organic phase was extracted with CH$_2$Cl$_2$ (3 times), dried over anhydrous sodium sulphate, and concentrated in a rotary evaporator. Without further purification, in a Schlenk flask, the alcohol (1 mmol) obtained in the previous step was subjected to the lactonization conditions along with trifluoroacetic acid (1.5 mmol) and dry dichloromethane (4 mL), for 24 hours at 40 °C, under an inert atmosphere. After this period, the reaction mixture was cooled and then neutralized with the addition of saturated sodium bicarbonate solution and extracted with dichloromethane (3 times). The organic phase was dried over anhydrous sodium sulphate and concentrated in a rotary evaporator in an ice bath. Purification of the product was done on a silica gel column using as an eluent solution 15% ethyl acetate: 85% hexane (v/v) for aromatic lactones and 10% petroleum ether: 90% dichloromethane for aliphatic lactones.

(E)-3-Ethylidenetetrahydro-2H-pyran-2-one (10E). CAS No [61203-10-9] physical state: yellow oil. Yield: 38%. ^{1}H NMR (600 MHz, CDCl$_3$, 25 °C) δ 7.14 (qt, J = 7.2, 2.4 Hz, 1H), 4.32–4.29 (m, 2H), 2.54–2.50 (m, 2H), 1.94 (dt, J = 11.1, 6.5 Hz, 2H), 1.79 (dt, J = 7.2, 1.4 Hz, 3H). ^{13}C NMR (151 MHz, CDCl$_3$, 25 °C) δ 166.7, 141.3, 126.5, 68.3, 23.6, 22.5, 14.2. MS (70 eV) *m/z*: 126 (M$^+$), 67 (100). IR (ATR): 2947, 1710, 1636, 1396, 1251, 1141, 1072. HRMS (ESI-TOF): [M + H]$^+$ calcd for C$_7$H$_{11}$O$_2$ 127.0754, found 127.0750.

(Z)-3-Ethylidenetetrahydro-2H-pyran-2-one (10Z). CAS No [61203-11-0] physical state: yellow oil. Yield: 18%. ^{1}H NMR (300 MHz, CDCl$_3$, 25 °C) δ 6.18 (qt, J = 7.2, 1.8 Hz, 1H), 4.30–4.24 (m, 2H), 2.61–2.52 (m, 2H), 2.10 (dt, J = 7.3, 1.8 Hz, 3H), 1.96–1.88 (m, 2H). ^{13}C NMR (75 MHz, CDCl$_3$, 25 °C) δ 165.9, 142.6, 125.7, 68.6, 29.1, 23.2, 16.2. MS (70 eV) *m/z*: 126 (M$^+$), 67 (100). IR (ATR): 2941, 1710, 1630, 1440, 1394, 1325, 1251, 1141, 1078.

HRMS (ESI-TOF): [M + H]$^+$ calcd for C$_7$H$_{11}$O$_2$ 127.0754, found 127.0752.

(E)-3-Propylidenetetrahydro-2H-pyran-2-one (11E). CAS No [98011-26-8] physical state: yellow oil. Yield: 67%. ^{1}H NMR (600 MHz, CDCl$_3$, 25 °C) δ 7.06–7.01 (m, 1H), 4.33–4.29 (m, 2H), 2.54–2.51 (m, 2H), 2.20–2.14 (m, 2H), 1.96–1.92 (m, 2H), 1.09–1.07 (m, 3H). ^{13}C NMR (75 MHz, CDCl$_3$, 25 °C) δ 166.8, 147.8, 125.0, 68.6, 23.7, 23.0, 21.6, 12.7. MS (70 eV) *m/z*: 140 (M$^+$), 67 (100). IR (ATR): 2970, 2866, 1710, 1636, 1383, 1302, 1244, 1153, 1089. HRMS (ESI-TOF): [M + H]$^+$ calcd for C$_8$H$_{13}$O$_2$ 141.0910, found 141.0920.

(Z)-3-Propylidenetetrahydro-2H-pyran-2-one (11Z). CAS No [98011-27-9] physical state: yellow oil. Yield: 10%. ^{1}H NMR (300 MHz, CDCl$_3$, 25 °C) δ 6.02 (tt, J = 7.2, 1.7 Hz, 1H), 4.29–4.23 (m, 2H), 2.60–2.50 (m, 4H), 1.97–1.86 (m, 2H), 1.03 (t, J = 7.5 Hz, 3H). ^{13}C NMR (75 MHz, CDCl$_3$, 25 °C) δ 165.8, 149.6, 124.1, 68.6, 29.3, 23.4, 23.2, 13.6. MS (70 eV) *m/z*: 140 (M$^+$), 67 (100). IR (ATR): 2964, 2878, 1705, 1630, 1389, 1239, 1141, 1066. HRMS (ESI-TOF): [M + H]$^+$ calcd for C$_8$H$_{13}$O$_2$ 141.0910, found 141.0919.

(E)-3-Heptylidenetetrahydro-2H-pyran-2-one (12E). CAS No [68872-81-1] physical state: yellow oil. Yield: 50%. ^{1}H NMR (600 MHz, CDCl$_3$, 25 °C) δ 7.06 (tt, J = 7.5, 2.4 Hz, 1H), 4.32–4.29 (m, 2H), 2.52 (t, J = 6.6 Hz, 2H), 2.14 (q, J = 7.4 Hz, 2H), 1.95–1.91 (m, 2H), 1.49–1.43 (m, 2H), 1.36–1.23 (m, 6H), 0.89 (t, J = 6.9 Hz, 3H). ^{13}C NMR (75 MHz, CDCl$_3$, 25 °C) δ 166.8, 146.8, 125.3, 68.5, 31.6, 29.0, 28.3, 28.1, 23.6, 22.6, 22.5, 14.0. MS (70 eV) *m/z*: 196 (M$^+$), 113 (100). IR (ATR): 2935, 2854, 1716, 1624, 1394, 1256, 1170. HRMS (ESI-TOF): [M + H]$^+$ calcd for C$_{12}$H$_{21}$O$_2$ 197.1542, found 197.1529.

(Z)-3-Heptylidenetetrahydro-2H-pyran-2-one (12Z). CAS No [68872-79-7] physical state: yellow oil. Yield: 10%. ^{1}H NMR (600 MHz, CDCl$_3$, 25 °C) δ 6.06 (tt, J = 7.2, 1.7 Hz, 1H), 4.30–4.28 (m, 2H), 2.63–2.57 (m, 4H), 1.96–1.93 (m, 2H), 1.33–1.30 (m, 6H), 0.90 (t, J = 7.0 Hz, 3H). ^{13}C NMR (75 MHz, CDCl$_3$, 25 °C) δ 165.9, 148.4, 124.5, 68.8, 31.6, 29.0, 28.3, 28.1, 23.4, 22.6, 22.5, 14.0. MS (70 eV) *m/z*: 196 (M$^+$), 139 (100). IR (ATR): 2965, 2936, 2876, 1715, 1635, 1396, 1236, 1139. HRMS (ESI-TOF): [M + H]$^+$ calcd for C$_{12}$H$_{21}$O$_2$ 197.1542, found 197.1530.

(E)-3-Octylidenetetrahydro-2H-pyran-2-one (13E) new compound. Physical state: yellow oil. Yield: 54%. ^{1}H NMR (600 MHz, CDCl$_3$, 25 °C) δ 7.06 (tt, J = 7.5, 2.3 Hz, 1H), 4.31–4.26 (m, 2H), 2.52 (m, 2H), 2.14 (q, J = 7.5 Hz, 2H), 1.94–1.93 (m, 2H), 1.31–1.27 (m, 11H), 0.88 (t, J = 7.0 Hz, 3H). ^{13}C NMR (151 MHz, CDCl$_3$, 25 °C) δ 166.7, 146.8, 125.3, 68.5, 31.7, 29.4, 29.1, 28.3, 28.1, 23.6, 22.7, 22.6, 14.1. MS (70 eV) *m/z*: 210 (M$^+$), 113 (100). IR (ATR): 2912, 2861, 1716, 1630, 1457, 1389, 1262, 1164, 1106, 1078. HRMS (ESI-TOF): [M + H]$^+$ calcd for C$_{13}$H$_{23}$O$_2$ 211.1698, found 211.1690.

(Z)-3-Octylidenetetrahydro-2H-pyran-2-one (13Z) new compound. Physical state: yellow oil. Yield: 26%. ^{1}H NMR (600 MHz, CDCl$_3$, 25 °C) δ 6.04 (tt, J = 7.2, 1.7 Hz, 1H), 4.28–4.25 (m, 2H), 2.64–2.53 (m, 4H), 1.96–1.88 (m, 2H), 1.46–1.38 (m, 2H), 1.35–1.21 (m, 9H), 0.88 (t, J = 7.1 Hz, 3H). ^{13}C NMR (151 MHz, CDCl$_3$, 25 °C) δ 166.3, 148.5, 124.7, 68.8, 31.8, 29.8, 29.4, 29.3, 29.3, 29.1, 23.4, 22.7, 14.1. MS (70 eV) *m/z*: 210 (M$^+$), 139 (100). IR (ATR): 2923, 2861, 1716, 1630, 1394, 1233, 1135. HRMS (ESI-TOF): [M + H]$^+$ calcd for C$_{13}$H$_{23}$O$_2$ 211.1698, found 211.1690.

(E)-3-(2-Methylpropylidene)tetrahydro-2H-pyran-2-one **(14E)** *new compound*. Physical state: yellow oil. Yield: 18%. ^{1}H NMR (600 MHz, CDCl$_3$, 25 °C) δ 6.89 (dt, J = 10.1, 2.3 Hz, 1H), 4.34–4.30 (m, 2H), 2.65–2.55 (m, 1H), 2.56 (td, J = 6.7, 2.3 Hz, 2H), 1.97–1.91 (m, 2H), 1.04 (d, J = 6.7 Hz, 6H). ^{13}C NMR (75 MHz, CDCl$_3$, 25 °C) δ 166.9, 152.4, 123.3, 68.4, 27.5, 23.3, 22.7, 21.4. MS (70 eV) m/z: 154 (M$^+$), 81 (100). IR (ATR): 2958, 2861, 1710, 1624, 1394, 1313, 1256, 1135. HRMS (ESI-TOF): [M + H]$^+$ calcd for C$_9$H$_{15}$O$_2$ 155.1072, found 155.1075.

(E)-3-Benzylidenetetrahydro-2H-pyran-2-one **(15E)**. CAS No [98011-25-7] physical state: yellow solid. Yield: 47%. ^{1}H NMR (600 MHz, CDCl$_3$, 25 °C) δ 7.93 (t, J = 2.3 Hz, 1H), 7.46–7.34 (m, 6H), 4.42–4.38 (m, 2H), 2.89 (dt, J = 6.59, 2.47 Hz, 2H), 2.00–1.95 (m, 2H). ^{13}C NMR (151 MHz, CDCl$_3$, 25 °C) δ 167.1, 141.5, 135.2, 130.3, 129.2, 128.7, 125.8, 68.8, 26.1, 23.2. MS (70 eV) m/z: 188 (M$^+$), 115 (100). IR (ATR): 2977, 1700, 1623, 1483, 1439, 1395, 1264, 1169, 1111. HRMS (ESI-TOF): [M + H]$^+$ calcd for C$_{12}$H$_{13}$O$_2$ 189.0916, found 189.0906.

(E)-3-(4-Chlorobenzylidene)tetrahydro-2H-pyran-2-one **(16E)**. CAS No [2409927-23-5] physical state: yellow solid. Yield: 45%. ^{1}H NMR (600 MHz, CDCl$_3$, 25 °C) δ 7.86 (s, 1H), 7.42–7.35 (m, 4H), 4.56–4.31 (m, 2H), 2.85 (td, J = 6.7, 2.2 Hz, 1H), 2.03–1.77 (m, 1H). ^{13}C NMR (151 MHz, CDCl$_3$, 25 °C) δ 166.6, 140.3, 135.1, 133.3, 131.6, 128.9, 126.3, 68.6, 25.8, 23.1. MS (70 eV) m/z: 188 (M$^+$), 115(100). IR (ATR): 2999, 2964, 2888, 1699, 1619, 1590, 1480, 1394, 1256, 1164, 822. HRMS (ESI-TOF): [M + H]$^+$ calcd for C$_{12}$H$_{12}$ClO$_2$ 223.0526, found 223.0533.

(E)-3-(4-Bromobenzylidene)tetrahydro-2H-pyran-2-one **(17E)**. CAS No [2639400-91-0] physical state: yellow solid. Yield: 52%. ^{1}H NMR (600 MHz, CDCl$_3$, 25 °C) δ 7.84 (t, J = 2.2 Hz, 1H), 7.57–7.54 (m, 2H), 7.32–7.28 (m, 2H), 4.43–4.39 (m, 1H), 2.84 (td, J = 6.6, 2.4 Hz, 1H), 2.03–1.96 (m, 1H). ^{13}C NMR (151 MHz, CDCl$_3$, 25 °C) δ 166.7, 140.1, 133.9, 131.8, 131.6, 126.5, 123.4, 68.7, 26.0, 22.9. MS (70 eV) m/z: 265 (M$^+$), 267 ((M+2)$^+$), 128 (100). IR (ATR): 2992, 2964, 2935, 2889, 2854, 1705, 1612, 1585, 1481, 1262, 1175. HRMS (ESI-TOF): [M + H]$^+$ calcd for C$_{12}$H$_{12}$^{79}BrO$_2$ 267.0021, found 266.9992.

(E)-3-(Benzo[d][1,3]dioxol-5-ylmethylene)tetrahydro-2H-pyran-2-one **(18E)**. CAS No [906423-89-0] physical state: yellow solid. Yield: 42%. ^{1}H NMR (600 MHz, CDCl$_3$, 25 °C) δ 7.83 (t, J = 2.1 Hz, 1H), 7.12–6.94 (m, 2H), 6.87 (d, J = 8.0 Hz, 1H), 6.03 (s, 2H), 4.47–4.34 (m, 2H), 2.87 (td, J = 6.7, 2.2 Hz, 2H), 2.09–1.94 (m, 2H). ^{13}C NMR (151 MHz, CDCl$_3$, 25 °C) δ 167.2, 148.5, 147.9, 141.4, 129.2, 126.0, 123.8, 109.8, 108.6, 101.5, 68.5, 26.1, 23.0. MS (70 eV) m/z: 232 (M$^+$), 148 (100). IR (ATR): 2970, 1681, 1590, 1509, 1452, 1273, 1239, 1164. HRMS (ESI-TOF): [M + H]$^+$ calcd for C$_{13}$H$_{13}$O$_4$ 233.0808, found 233.0811.

(E)-3-(4-Nitrobenzylidene)tetrahydro-2H-pyran-2-one **(19E)**. CAS No [1334334-84-7] physical state: yellow solid. Yield: 20%. ^{1}H NMR (300 MHz, CDCl$_3$, 25 °C) δ 8.32–8.23 (m, 1H), 7.93 (t, J = 2.4 Hz, 1H), 7.61–7.54 (m, 2H), 4.49–4.40 (m, 2H), 2.87 (td, J = 6.6, 2.5 Hz, 2H), 2.05–1.97 (m, 2H). ^{13}C NMR (75 MHz, CDCl$_3$, 25 °C) δ 165.9, 141.2, 138.8, 130.6, 129.5, 123.7, 68.6, 25.83, 23.0. MS (70 eV) m/z: 232 (M$^+$), 115 (100). IR (ATR): 2970, 1699, 1515, 1331, 1164, 1112, 1066. HRMS (ESI-TOF): [M + H]$^+$ calcd for C$_{12}$H$_{12}$NO$_4$ 234.0766, found 234.0779.

Synthesis for chlorolactone (20). This known inhibitor was synthesized according to the methodology of Bassler and co-workers with modifications.[34] In a 100 mL flask, 1.8 g of *p*-chlorophenol (S1, 14 mmol) and 3.8 g of potassium carbonate (28 mmol) were added. The atmosphere was exchanged for N$_2$ and 2.0 mL of ethyl 4-bromobutanoate (S2, 14 mmol), and 40 mL of dry DMF were added. The flask was closed with a reflux condenser connected to a calcium chloride tube, and the reaction was heated to 140 °C for 4 hours. After cooling, the reaction was diluted with 100 mL of distilled water and extracted with 4 × 30 mL of hexane. The organic phase was dried with Na$_2$SO$_4$ and the solvent was removed on a rotary evaporator, resulting in 3.4 g (14 mmol, quantitative yield) of an oil characterized as S3. Two grams of S3 were saponified with 34 mL of a solution of methanol and 1 M NaOH (1 : 1 v/v), under stirring for 18 hours at room temperature. Then, the reaction was acidified to pH = 1 with 1 M HCl, and a white solid was filtered through a Büchner funnel, yielding 1.7 g (7.9 mmol, 86% yield) of a solid characterized as S4.† A solution of 0.5 g of S4† (2 mmol) with 0.4 g of 1-ethyl-3-(3-dimethyl aminopropyl) carbodiimide hydrochloride (EDC·HCl, 2 mmol) in 20 mL of dry dichloromethane was prepared in a 50 mL flask under inter atmosphere. The reaction was stirred for 5 minutes at 0 °C. To this mixture, 2.3 mmol of lactone and 1.3 mL of Et$_3$N (9.3 mmol) were added. The reaction was left under stirring for an additional 1 hour at 0 °C and 18 hours at room temperature. The reaction was then washed with 5 × 20 mL of HCl (1 M), and 5 × 20 mL of a saturated solution of NaHCO$_3$. The organic phase was dried with Na$_2$SO$_4$ and the solvent was removed on a rotary evaporator. Purification was done on a silica gel column (dichloromethane/ethyl acetate 2 : 0.5). The fractions were collected, and the solvent was removed on a rotary evaporator. Then, the material was submitted to a high vacuum to remove any residual solvent, yielding 0.41 mg (1.4 mmol, 61% yield) of a solid characterized as a known inhibitor, **20**.

(S)-4-(4-Chlorophenoxy)-N-(2-oxotetrahydrofuran-3-yl)butanamide **(20)**. CAS No [1453857-28-7] ^{1}H RMN (600 MHz, CDCl$_3$, 25 °C): δ 7.24–7.20 (m, 2H), 6.84–6.79 (m, 2H), 6.23 (d, J = 5.4 Hz, 1H), 4.56 (ddd, J = 11.6, 8.6, 6.1 Hz, 1H), 4.48–4.44 (m, 1H), 4.28 (ddd, J = 11.2, 9.3, 5.9 Hz, 1H), 3.98 (td, J = 6.1, 1.5 Hz, 2H), 2.84–2.77 (m, 1H), 2.47 (dd, J = 10.8, 4.1 Hz, 2H), 2.13 (ddd, J = 13.3, 7.2, 6.2 Hz, 3H). ^{13}C RMN (151 MHz, CDCl$_3$, 25 °C): δ 175.4, 172.9, 157.3, 129.3, 125.7, 115.7, 67.0, 66.0, 49.2, 32.3, 30.4, 24.8. EM (70 eV) m/z: 170 (100). IR (ATR) cm^{-1}: 3291, 1767, 1643, 1540, 1493, 1243, 1189, 660.

Bacterial strains and growth conditions

C. subtsugae strain CV026 (AHL-deficient mutant of *C. subtsugae* strain ATCC 31532 – genotype cviI : mini-Tn5, Km^r, AHL$^-$) was kept under cryopreservation (−80 °C) in LB medium supplemented with 50% glycerol. CV026 was recovered with kanamycin (50 µg mL^{-1}) and cultured in LB broth (pH 7.2) under stirring at 200 rpm for 24 hours at 28 °C. To obtain isolated colonies, LB agar supplemented with HHL (**2**) (4 nM) was streaked with 10 µL of bacterial culture and incubated at 28 °C for 48 h. Isolated CV026 colonies were surveyed for the steady production of violacein.

Violacein quantification assay

Isolated colonies of CV026 (LB agar – 48 hours at 28 °C) were used to make a bacterial suspension in LB medium adjusted to 2.0 McFarland scale. The bacterial suspension was used to inoculate the test medium in a proportion of 10% v/v. The test medium was then supplemented with the cognate autoinducer (N-hexanoyl-L-homoserine 96% lactone, Sigma-Aldrich), at a final concentration of 10 μM. A 1.95 mL aliquot of this culture was transferred to a conical falcon tube ($v = 15$ mL) and supplemented with 50 μL of the tested molecules in an acetone solution of 25%, in different final concentrations (2.5 mM, 1.25 mM, 625 μM and 312 μM). The assays were incubated under agitation at 200 rpm at 30 °C for 24 hours and then were put in a kiln to completely evaporate the liquid medium. Violacein was solubilized from dried bacterial pellets with 1 mL of DMSO. After 24 h of agitation, the absorbance of soluble violacein was measured at 630 nm using a microplate reader (Biotek – ELx808™).

The same experimental conditions were repeated, in parallel, in the absence of the cognate auto-inducer ("blank") for evaluating the bacterial growth by measuring turbidity (630 nm) after 24 hours under agitation at 200 rpm and 30 °C in a microplate reader (Biotek – ELx808™).

Competitive assay

Competition assays for the CviR binding site were performed following the same set-up as the violacein quantification assay, but adopting different concentrations of the cognate AI, **1**, (10 nm to 1 mM) and a fixed concentration of lactone **20** (312 μM).

Chitinase assay on agar plates

The protocol established by Chernin *et al.* for testing chitin hydrolysis in *Chromobacterium* CV026 was conducted with minor modifications. Isolated colonies of CV026 (LB agar – 48 hours at 28 °C) were used to make a bacterial suspension in NaCl 0.9% (w/w) medium adjusted to 2.0 McFarland scale. A 10 μL aliquot of this suspension was placed onto plates with a semi-minimal medium consisting of 10% LB (v/v), 0.2% (w/v) colloidal chitin[32] and supplemented with HHL at a final concentration of 10 μM (positive control of chitinase hydrolysis – PC). A plate without HHL was made for the negative control of chitinase hydrolysis (NC). **20** and **15E** were evaluated in chitinase hydrolysis assay. In the test medium, the respective molecules were added at the final concentrations of 32 μM for **20** and 312 μM for **15E**. The plates were incubated at 30 °C for 72 hours until zones of clearing of the chitin could be seen around the colonies.

RT-qPCR assays

Total RNA was extracted from CV026 cells in the same condition as in the violacein quantification assay using the ReliaPrep™ RNA Miniprep System (Promega) as indicated by the manufacturer's instructions. Primers for *vioA*, *vioC*, and *gyrB* were designed using the web-based tool Primer-BLAST (https://www.ncbi.nlm.nih.gov/tools/primer-blast) (Table 3).[37]

Table 3 Primer sequence used in Rt-qPCR

Primer	Sequence
vioA-F	ATCCGGAAATCCAGAGCTTC
vioA-R	ACTTGTCGCCCTTGAAGTAG
vioC-F	GCCTTTTTCGACCGTTACTTC
vioC-R	CTATGCATGTAGCGGGTGTA
gyrB-F	TCACCATCAATCCGGACAAC
gyrB-R	TCTTGTTGCGGTTCATGTATTC

Total RNA was used as a template for the reverse transcription reaction using the GoTaq® 1-Step RT-qPCR System (Promega). The RT-qPCR was performed in one step according to the manufacturer's protocol. The reaction mix (20 μL) was made up as follows: 10 μL GoTaq® qPCR Master Mix, 2.5 μL forward and reverse primers (150 nM), 0.4 μL GoScript™ RT Mix for 1-Step RT-qPCR and 4 μL of the RNA template (20 ng). RT-qPCR was performed using Applied Biosystems Quant Studio™ 3 Real-Time PCR System (Applied Biosystems Inc., CA, USA). The reaction conditions are as follows: reverse transcriptase reaction at 37 °C for 15 minutes, RT enzyme inactivation at 95 °C for 10 minutes, followed by 40 cycles of denaturation at 95 °C for 10 s, annealing at 54 °C for 30 s and extension at 72 °C for 30 s. The relative mRNA expression of *vioA* and *vioC* was calculated using the $\Delta\Delta Ct$ method. *gyrB* was used as an internal reference gene for normalization. These experiments were independently conducted 3 times.

Evaluation of the antagonistic activity of compounds 9–21 through molecular docking analysis

In this study, AutoDock Vina 1.1.2 and VMD 1.9.3 (ref. 35 and 38) programs were used for molecular docking and visualization. Molecular docking was used for the prediction of the interaction between the possible QSI and CviR. The structures of the molecules were optimized using density functional theory at B3LYP/6-311G (d,p) level in Gaussian 6.06.[39] The enzyme structure of CviR (PDB ID 3QP5) was obtained from the RCSB protein data bank (https://www.rcsb.org/) and the molecular docking studies were carried out using the dimer structure. The grid box center was set at the centre of the dimer ($x = 39$, $y = -0.15$, $z = 15.71$), and the dimensions of the box were set at 60 Å × 90 Å × 100 Å. The docking results are a list of the free energy of binding (ΔG) of the protein and molecules binding poses. This can be considered as a measure of a predicted binding affinity in kcal mol^{-1}. Last, the complex structures were evaluated using VMD 1.9.3 program, and the distance between the molecules and the amino acids was measured.

Redocking was used to ensure that this computational tool was able to mimic the interactions between ligand and protein. The overlap between the chlorolactone pose from the X-ray crystal structure and the docking one (Fig. S17†) is considered good for determining docking as an accurate computational predictor of interactions between ligand and protein. Molecule

21 had no interaction within the binding site, as seen in Fig. S32,† even when the grid box was reduced to the AIBD size.

It is important to mention that we were careful to use the correct pdb for the strain tested. The 3QP5 pdb file is the crystallographic structure of the X-ray of the CviR complex with the *Chlorolactone* **20** (*C. subtsugae* ATCC 31532/CV026).

LogP

Chemicalize was used for the prediction of log*P*. https://chemicalize.com/developed by ChemAxon (https://www.chemaxon.com).

Author contributions

W. T., A. L. P. and A. H. L. M. designed the research. F. F. and T. A. T. performed the synthetic chemistry research. F. F. performed the biological assays, and the computational biology research. F. F., T. A. T., V. F., W. T., A. L. P. and A. H. L. M. analysed the data. F. F., A. L. P. and A. H. L. M. wrote the paper. T. A. T., V. F., W. T., A. L. P. and A. H. L. M. revised the manuscript.

Conflicts of interest

There are no conflicts to declare.

Acknowledgements

Notes and references

1 H. M. C. Ferraz, F. I. Bombonato, M. K. Sano and L. S. Longo, *Quim. Nova*, 2008, **31**, 885.
2 S. L. Robinson, J. K. Christenson and L. P. Wackett, *Nat. Prod. Rep.*, 2019, **36**, 458.
3 A. Albrecht, J. F. Koszuk, J. Modranka, M. Różalski, U. Krajewska, A. Janecka, K. Studzian and T. Janecki, *Bioorg. Med. Chem.*, 2008, **16**, 4872.
4 T. Janecki, *Natural Lactones and Lactams: Synthesis, Occurrence and Biological Activity*, Wiley-VCH, Weinheim, 2014.
5 S. Mukherjee and A. T. Biju, *Chem.–Asian J.*, 2018, **13**, 2333.
6 D. M. Souza, L. L. Machado and A. H. L Machado, *Tetrahedron Lett.*, 2019, **60**, 1811–1813.
7 M. Whiteley, S. Diggle and E. Greenberg, *Nature*, 2017, **551**, 313–320.
8 A. Camilli and B. B. Bassler, *Science*, 2006, **311**, 1113–1116.
9 M. Thoendel, J. S. Kavanaugh, C. E. Flack and A. R. Horswill, *Chem. Rev.*, 2011, **111**, 117–151.
10 X. Huang, O. P. Duddy, J. E. Silpe, J. E. Paczkowski, J. Cong, B. R. Henke and B. L. Bassler, *J. Biol. Chem.*, 2020, **295**, 291.
11 A. G. Palmer, A. C. Senechal, T. C. Haire, N. P. Mehta, S. D. Valiquette and H. E. Backwell, *ACS Chem. Biol.*, 2018, **13**, 31115–31122.
12 X. Zhao, Z. Yu and T. Ding, *Microorganisms*, 2020, **8**, 425.
13 G. Chen, L. R. Swem, D. L. Swem, D. L. Stauff, C. T. O'Loughlin, P. D. Jeffrey, B. L. Bassler and F. M. Hughson, *Mol. Cell*, 2011, **42**, 199.
14 S. Haque, D. K. Yadav, S. C. Bisht, N. Yadav, V. Singh, K. K. Dubey, A. Jawed, M. Wahid and S. A. Dar, *J. Chemother.*, 2019, **31**, 161.
15 L. Lu, M. Li, G. Yi, L. Liao, Q. Cheng, J. Zhu, B. Zhang, Y. Wang, Y. Chen and M. Zeng, *J. Pharm. Anal.*, 2021, **12**, 1.
16 B. Rémy, S. Mion, L. Plener, M. Elias, E. Chabrière and D. Daudé, *Front. Pharmacol.*, 2018, **9**, 203.
17 E. Shaw and W. M. Wuest, *RSC Med. Chem.*, 2020, **11**, 358.
18 P. Piewngam, J. Chiou, P. Chatterjee and M. Otto, *Expert Rev. Anti-Infect. Ther.*, 2020, **18**, 499.
19 M. E. Mattmann and H. E. Blackwell, *J. Org. Chem.*, 2010, **75**, 6737.
20 T. Zang, B. W. K. Lee, L. M. Cannon, K. A. Ritter, S. Dai, D. Ren, T. K. Wood and Z. S. Zhou, *Bioorg. Med. Chem. Lett.*, 2009, **19**, 6200.
21 S. Manner and A. Fallarero, *Int. J. Mol. Sci.*, 2018, **19**, 1346.
22 O. M. Vandeputte, M. Kiendrebeogo, T. Rasamiravaka, C. Stévigny, P. Duez, S. Rajaonson, B. Diallo, A. Mol, M. Baucher and M. el Jaziri, *Microbiology*, 2011, **157**, 2120.
23 K. H. McClean, M. K. Winson, L. Fish, A. Taylor, S. R. Chhabra, M. Camara, M. Daykin, J. H. Lamb, S. Swift, B. W. Bycroft, G. S. A. B. Stewart and P. Williams, *Microbiology*, 1997, **143**, 3703.
24 G. Devescovi, M. Kojic, S. Covaceuszach, M. Cámara, P. Williams, I. Bertani, S. Subramoni and V. Venturi, *Front. Microbiol.*, 2017, **8**, 349.
25 A. M. Harrison and S. D. Soby, *AMB Express*, 2020, **10**, 202.
26 T. Hoshino, *Appl. Microbiol. Biotechnol.*, 2011, **91**, 1463–1475.
27 N. Durán, G. Z. Justo, M. Durán, M. Brocchi, L. Cordi, L. Tasic, G. R. Castro and G. Nakazato, *Biotechnol. Adv.*, 2016, **34**, 1030.
28 A. Chang, S. Sun, L. Li, X. Dai, H. Li, Q. He and H. Zhu, *Bioorg. Chem.*, 2019, **91**, 103140.
29 X. Zhuang, A. Zhang and W. Chu, *Int. Microbiol.*, 2020, **23**, 215.
30 R. E. D'Almeida, R. D. I. Molina, C. M. Viola, M. C. Luciardi, C. Nieto Peñalver, A. Bardón and M. E. Arena, *Bioorg. Chem.*, 2017, **73**, 37.
31 A. Albrecht, Ł. Albrecht and T. Janecki, *Eur. J. Org. Chem.*, 2011, 2747.
32 L. S. Chernin, M. K. Winson, J. M. Thompson, S. Haran, B. W. Byceoft, I. Chet, P. Willians and G. S. A. B. Stewart, *J. Bacteriol.*, 1998, **180**, 4435–4441.
33 V. S. Silva, T. A. Tolentino, T. C. A. F. Rodrigues, F. F. M. Santos, D. F. S. Machado, W. A. Silva, H. C. B. De Oliveira and A. H. L. Machado, *Org. Biomol. Chem.*, 2019, **17**, 4498.

34 L. R. Swem, D. L. Swem, C. T. O'Loughlin, R. Gatmaitan, B. Zhao, S. M. Ulrich and B. L. Bassler, *Mol. Cell*, 2009, **35**, 143.

35 O. Trott and A. J. Olson, *J. Comput. Chem.*, 2010, **31**, 455.

36 C. Vraka, L. Nics, K. H. Wagner, M. Hacker, W. Wadsak and M. Mitterhauser, *Nucl. Med. Biol.*, 2017, **50**, 1.

37 J. Ye, G. Coulouris, I. Zaretskaya, I. Cutcutache, S. Rozen and T. L. Madden, *BMC Bioinf.*, 2012, **13**, 134.

38 W. Humphrey, A. Dalke and K. Schulten, *J. Mol. Graphics*, 1996, **14**, 33.

39 M. J. Frisch, G. W. Trucks, H. B. Schlegel, G. E. Scuseria, M. A. Robb, J. R. Cheeseman, G. Scalmani, V. Barone, G. A. Petersson, H. Nakatsuji, X. Li, M. Caricato, A. V. Marenich, J. Bloino, B. G. Janesko, R. Gomperts, B. Mennucci, H. P. Hratchian, J. V. Ortiz, A. F. Izmaylov, J. L. Sonnenberg, D. Williams-Young, F. Ding, F. Lipparini, F. Egidi, J. Goings, B. Peng, A. Petrone, T. Henderson, D. Ranasinghe, V. G. Zakrzewski, J. Gao, N. Rega, G. Zheng, W. Liang, M. Hada, M. Ehara, K. Toyota, R. Fukuda, J. Hasegawa, M. Ishida, T. Nakajima, Y. Honda, O. Kitao, H. Nakai, T. Vreven, K. Throssell, J. A. MontgomeryJr, J. E. Peralta, F. Ogliaro, M. J. Bearpark, J. J. Heyd, E. N. Brothers, K. N. Kudin, V. N. Staroverov, T. A. Keith, R. Kobayashi, J. Normand, K. Raghavachari, A. P. Rendell, J. C. Burant, S. S. Iyengar, J. Tomasi, M. Cossi, J. M. Millam, M. Klene, C. Adamo, R. Cammi, J. W. Ochterski, R. L. Martin, K. Morokuma, O. Farkas, J. B. Foresman and D. J. Fox, *Gaussian 16, Revision C.01*, Gaussian, Inc., Wallingford CT, 2016.